

Comparison of magnetic resonance imaging of the prostate 1.5T and 3T

Goran Kutlić^{1,2}, Krešimir Dolić^{2,3,4}

¹ University Hospital "Holy Spirit", Zagreb, Croatia

² University Department of Health Studies, University of Split, Split, Croatia

³ Department of Diagnostic and Interventional Radiology, University Hospital of Split, Split, Croatia

⁴ School of Medicine, University of Split, Split, Croatia

Corresponding author: Goran Kutlić, e-mail: gorankutlic@proton.me

DOI: <https://doi.org/10.55378/rv.49.1.5>

Abstract

With its excellent display of soft tissues and the possibilities of three-dimensional display, magnetic resonance has become one of the fundamental diagnostics in the display of prostate and its pathological conditions since its beginnings 40 years ago. Although there is greater availability of devices for magnetic resonance with a field strength of 1.5T, the recommendation of the European Association of Urogenital Radiologists is that imaging of the prostate with magnetic resonance is performed on devices with a field strength of 3T. 3T devices were introduced due to the increased signal-to-noise ratio (SNR), which can be used to shorten recording time or increase resolution, i.e. improve image quality. There is more and more research into the application of quantitative techniques such as Magnetic resonance fingerprinting, T2 mapping, BOLD, which could improve the detection and quantification of prostate cancer lesions, and by optimizing the protocol at 1.5T and 3T it is possible to perform exam of equal diagnostic value.

Keyword: MRI; prostate; 1.5T; 3T

Introduction

Magnetic resonance imaging (MRI) of the prostate is a diagnostic method for detecting and assessing the extent of benign and malignant changes in the prostate. The examination is performed on 1.5T and 3T devices with an abdominal coil or with the use of an endorectal coil (ERC).

Although 1.5T and 3.0T field strength devices for prostate imaging can provide adequate and reliable diagnostic examinations when acquisition parameters are optimized and appropriate modern technology is used, according to the Prostate Imaging-Reporting and Data System (PI-RADS) v2.1 document, it is recommended that MRI of the prostate, if possible, be performed on 3T field strength devices due to better signal-to-noise ratio (SNR), spatial and temporal resolution. Devices with a field strength of 1.5T are recommended in cases where the patient has implants that are conditioned for a field strength of 1.5T. They are also recommended in cases where the implants are safe for the 3T field strength, but are anatomically located in such a way that they will cause artifacts that will affect the quality of the examination. Performing the search on devices with a field strength of less than 1.5T is not recommended [1].

In prostate imaging, biparametric (bpMRI) or multiparametric (mpMRI) protocols are used, which include: T1 weighted image (T1W), T2 weighted image (T2W), dif-

fusion weighted images (DWI), sequences with dynamic contrast (DCE) and in some cases spectroscopy.

Over the last 10 years, advances in mpMRI have made it possible to accurately detect and characterize lesions suspected of prostate cancer. The widespread use of prostate mpMRI has resulted in high variability in scan quality for each sequence, and especially for DWI and DCE sequences [2].

In the last 5 years, several debates have been initiated about the best protocol for prostate MRI to obtain adequate diagnostic quality with good spatial resolution and high signal-to-noise ratio for each sequence. Currently, the recommendation of the PI-RADS v2.1 document is a minimum T2W sequence in the axial plane and additionally in the sagittal or coronary plane, DWI sequences and DCE sequences (Figure 1.) [3].

Aim

The aim of this paper is to present the current research of prostate MRI in clinical practice on devices with a field strength of 1.5T and 3T.

The paper was made by searching scientific papers in the PubMed database in the period from year 2012 till 2023. The terms MRI, prostate, 1.5T, 3T were used for the examination. The search yielded 305 published scientific

| | T2-weighted imaging (T2-WI) | Diffusion-weighted imaging (DWI) | Dynamic contrast-enhanced (DCE) |
|------------------------------------|---|---|---------------------------------|
| Imaging planes | Same used for DUT and DCE | Same used for T2-UT and DCE | Same used for T2- UT and DUT |
| Slice thickness | 3 mm no gap | <4 mm. no gap | 3 mm no gap |
| Field of new | 12–20 cm | 16–22 cm | 12–20 cm |
| In-plane dimension | <0.7 mm (phase)×≤ 0.4 mm (frequency) | <2.5 mm (phase and frequency) | <2 mm (phase and frequency) |
| Specific recommendations | | | |
| T2-WI acquisition | Axial plane: either straight axial to the patient or in an oblique axial plane matching the long axis of the prostate | - | - |
| | At least one additional orthogonal plane (sagittal and/or coronal) | - | - |
| | 3D axial as an adjunct to 2D acquisitions | - | - |
| Low <i>b</i>-value | - | 0 (preferably 50)–100 sec/mm ² | - |
| Intermediate <i>b</i>-value | - | 800–1000 sec/mm ² | - |
| High <i>b</i>-value | - | <ul style="list-style-type: none"> ● Dedicated (≥1,400 sec/mm²) • Synthesised (from other <i>b</i>-values) | - |
| Temporal resolution | - | - | ≤15 s |
| Total observation rate | - | - | >2 min |
| Dose of GBCA | - | - | 0.1 mmol/kg |
| Injection rate | - | - | 2 – 3cc/s |
| Fat suppression/subtraction | - | - | Recommended |

Figure 1. Minimum technical requirements for mpMRI according to PI-RADS v2.1 guidelines

Source: <https://www.acr.org/-/media/ACR/Files/RADS/PI-RADS/PIRADS-v2-1.pdf>

papers, whereby 23 of them were selected based on predetermined criteria and were used in the writing of this paper.

Methods

According to the current recommendations of the American College of Radiology (ACR) and the European Society of Urogenital Radiology (ESUR) published in the guidelines PI-RADS v2.1, T1W, T2W, DWI sequences are required for

all MRI examinations of the prostate and, if necessary, DCE sequence and spectroscopy are used [1].

T1W sequences are primarily used to determine the presence of bleeding inside the prostate and seminal vesicles and to show, i.e. outline of the prostate (Figure 2.).

T1W sequences may also be useful for detecting nodal and skeletal metastases, especially after intravenous administration of a gadolinium-based contrast agent (Figure 2.). Axial T1W images of the prostate can be obtained with or without fat suppression using spin echo or

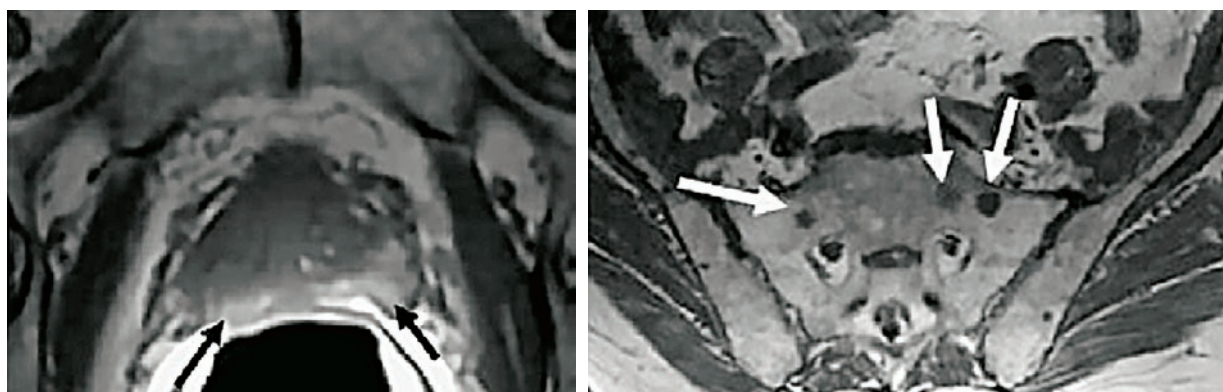


Figure 2. on the left is T1W image of bleeding after biopsy and right is T1W image of metastases in the sacrum

Source: https://www.researchgate.net/publication/6352762_Prostate_cancer_detection_Magnetic_resonance_MR_spectroscopic_imaging/figures?lo=1

gradient echo sequences. The recording planes should be the same as those used for DWI and DCE. Unlike the T2W sequence, in which spatial resolution is important, in the T1W sequence, temporal resolution is more important. Thus, in the T1W sequence, we can reduce spatial resolution and use this to increase anatomical coverage [4].

In MRI examination of the prostate, T2W images are used to discern the zonal anatomy of the prostate, assess abnormalities within the gland, and assess the involvement of seminal vesicles and node involvement.

On T2W images, carcinomas in the peripheral zone usually appear as round and poorly defined hypointense focal lesions. Also, hypointense displays can have conditions such as prostatitis, bleeding, atrophy of the glands, benign hyperplasia, scars associated with biopsy and after therapy (hormonal, ablation, etc.). Transitional zone carcinomas can be difficult to identify on T2W images because the transition zone often consists of varying amounts of intermixed glandular (T2-hyperintense) and stromal (T2-hypointense) tissue, which shows a heterogeneous signal intensity. Areas where benign stromal elements predominate may mimic and/or mask clinically significant cancers.

T2W images should always be obtained in the axial plane and at least one additional orthogonal plane (i.e., sagittal and/or coronal). T2W images are usually obtained using two-dimensional (2D) FSE or TSE techniques.

According to the recommendation of PI-RADS v2.1, the parameters that should be followed are as follows:

- slice thickness: 3 mm, without gaps,
- The recording planes must be identical to those of the DWI and DCE sequences,
- FOV: generally 12-20 cm to cover the entire prostate and seminal vesicles,
- In-plane: ≤ 0.7 mm (phase) x ≤ 0.4 mm (frequency).

Also, further improvement of T2W sequences is achieved by optimizing parameters such as: TSE factor, TSE spacing and choice of image filters [5].

Three-dimensional (3D) imaging can be used in addition to two-dimensional (2D) imaging. If recorded using isotropic voxels, 3D images can be particularly useful for visualizing detailed anatomy and distinguishing between true lesions and partial volume averaging effects. However, the contrast of the soft tissue is not identical and, in some cases, may be worse than that seen in 2D T2W images, and the resolution in the plane may be lower than the 2D image taken with the same technique (Figure 3.).



Figure 3. T2W axial showing prostate cancer

Source: <https://radiologyassistant.nl/abdomen/prostate/prostate-cancer-pi-rads-v2>

Diffusion-weighted imaging (DWI) reflects the random movement of water molecules and is a key component of the mpMRI prostate imaging protocol. Most clinically significant cancers have limited diffusion as compared to normal tissues, hence they appear hypointense on the greyscale ADC maps. Although ADC values have been reported to be inversely correlated with histological grades, there is significant overlap between BPH, low-grade cancer, and high-grade cancer.

According to the recommendations of PI-RADS v2.1, an ADC map and images with a high b-value ($b > 1400$ s/mm²) should be included. An ADC map is a representation of the ADC value for each voxel in an image. In most current clinical implementations, two or more b-values and a mono exponential signal attenuation model with increasing b-values are used to calculate ADC values. ADC calculations are influenced by the selection of b-values and are not standardized among device manufacturers. Independent of devices, qualitative visual assessment is most commonly used as the primary method for assessing ADCs. If we use ADC values of 750-900 $\mu\text{m}^2/\text{sec}$, we can differentiate a benign lesion from prostate cancer. Images with a high b-value are considered to be those with at least 1400 s/mm². They show signal conservation in areas of limited/prevented diffusion compared to normal tissues. Normal tissues show a reduced signal due to greater diffusion between the application of gradients with different b-values. Compared to the basic ADC maps alone (b-value 0-100 s/mm² and 800-1000 s/mm²), the visibility of clinically significant cancers is sometimes improved in high-b-value images. Especially on those that are adjacent to the anterior fibromuscular stroma [6]. Increasing the b-value above 3000 s/mm² has been shown to better suppress the background signal, but does not contribute to improved prostate cancer detection [7]. High-b-value images can be obtained in one of two ways: directly by obtaining a high-b-value DWI sequence, or by calculating a high-b-value image from the collected data of lower b-value DWI sequences.

Recommended parameters for DWI sequences according to PI-RADS v2.1:

- SE EPI sequence without retention of breathing and fat saturation,
- TE: ≤ 90 msec; TR: ≥ 3000 msec,
- slice thickness: ≤ 4 mm, without gaps,
- the image planes should match or be similar to those used for T2W and DCE sequences,
- FOV: 16-22 cm,
- plane dimensions: ≤ 2.5 mm phase and frequency,
- in case of time or technical limitation of the MRI device, it is recommended to use two values, one low b-value of 50-100 s/mm² and one medium b-value of 800-1000 s/mm²,
- it is recommended that the maximum b-value used for the calculation of the ADC be ≤ 1000 s/mm² in order to avoid the diffusion kurtosis effect that is described at higher b-values,
- Images with a high B-value (≥ 1400 s/mm²) are also mandatory and should preferably be obtained through a separate acquisition.

DCE MRI is defined as obtaining T1W gradient echo scans before, during, and after intravenous administration of a gadolinium-based contrast agent. After contrast administration, prostate cancer tissue shows an early im-

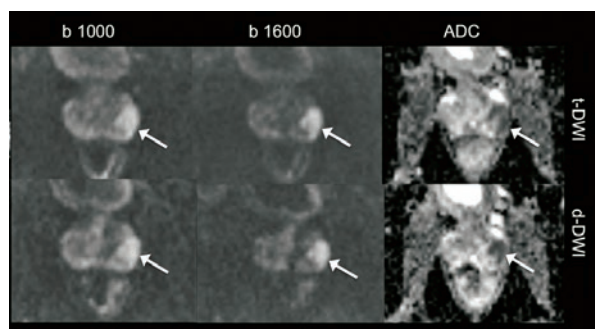


Figure 4. Example of DWI sequences and ADC maps of prostate cancer

Source: <https://onlinelibrary.wiley.com/doi/10.1002/jmri.25705>

provement in signals compared to normal tissue. DCE is performed in multiple repeated series of signal acquisition to show early lesions compared to surrounding prostate tissue. It is carried out for several minutes in order to evaluate the characteristics of signal improvement. DCE sequences should have a time resolution of <15 seconds per recording to show focal early signal gain. Likewise, a faster temporal resolution can be selected if we maintain sufficient spatial resolution and diagnostic image quality. The diagnostic quality of the image can be further improved by suppression of fat signals or subtraction. 3D T1W sequences on the new devices have reached the quality of 2D T1W sequences and it is recommended to use them in order to shorten the review time.

Parameters for DCE sequences are:

- TR/TE: <100 msec/ <5 msec
- layer thickness: 3 mm, no gaps
- acquisition planes identical to DWI
- FOV: covers the entire prostate and seminal vesicles
- total recording duration: >2 min,
- Dose: 0.1 mmol/kg standard contrast based on gadolinium,
- Contrast application speed: 2-3 cc/s, and the start of administration correlates with the initiation of the sequence.

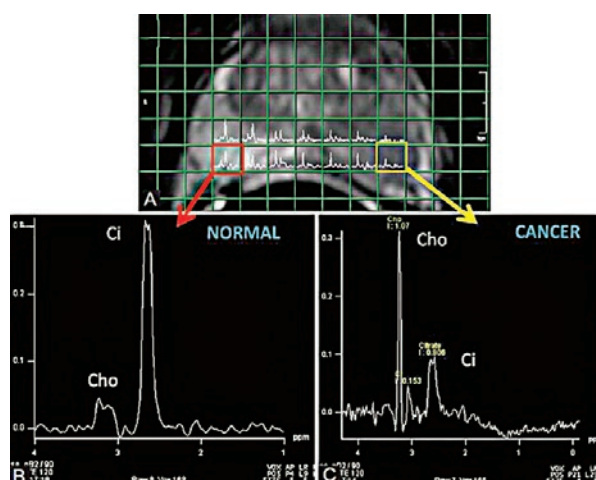


Figure 5. An example of MR spectroscopy where the left is the spectroscopy of the normal prostate and the right is the prostate cancer spectroscopy

Source: <https://mriquestions.com/prostate-spectra.html>

Spectroscopy is a non-invasive method based on spectroscopic analysis of tissue metabolism and as such is used to characterize metabolic changes associated with prostate cancer. Prostate spectroscopy is based on measurements of citrate, choline and creatinine concentrations. Although it used to be the standard method for MRI imaging of the prostate, today spectroscopy is according to PI-RADS v2.1. auxiliary method [1]. MRI prostate spectroscopy was the first method of choice for detecting aggressive cancers. By improving DWI sequences, we can now collect the same information in a shorter time and in a more technically simpler way (Figure 5.) [6].

New paths in MRI prostate

3D T2W Sequence

Three-dimensional imaging allows visualization of the prostate in any arbitrarily determined anatomical plane, without loss of image quality, and can be obtained in a shorter time compared to separate multiplanar 2D imaging [8]. High-resolution 3D T2W MRI with adequate volumetric coverage can improve sensitivity for cancer detection [9]. It allows for a more accurate image-guided biopsy and improves surgical planning or targeted treatment. The 3D sequence can be optimally used in the latest technologies such as PET-MR, whereby fast 3D T2W MRI sequences are used to fuse the image with 3D PET (Figure. 6.) [10].

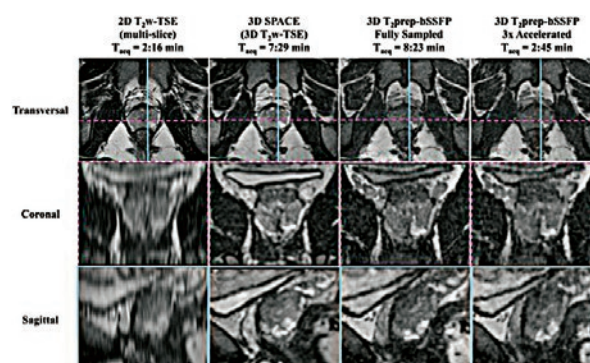


Figure 6. Comparison of 2D T2W and 3D T2W sequences with acquisition time

Source: <https://www.ncbi.nlm.nih.gov/pmc/articles/instance/6563534/bin/MRM-82-721-g004.jpg>

Functional magnetic resonance imaging (fMRI)

fMRI is a rapid MRI technique that obtains images of organs in the activity phase and then in the resting phase. In prostate imaging, the Blood oxygenation level dependent (BOLD) sequence is based on the difference in magnetic sensitivity of oxyhemoglobin and deoxyhemoglobin due to increased blood flow in the vessels and reduced or no increase in local oxygen consumption that occurs during activity [11]. In the case of prostate cancer, it is known that in solid fast-growing tumors, there is a decrease in oxygen levels in the tissues due to inadequate blood supply and too rapid tumor growth. If we apply the BOLD

technique, we can quantify the distribution of cancer in the prostate. Since deoxyhemoglobin is paramagnetic, the vessels containing a significant amount of this molecule generate local field inhomogeneities causing dephasing and, therefore, signal loss. During activity, there is an increase in blood supply to the prostate tissue, and thus the level of deoxyhemoglobin decreases, resulting in an increase in signal intensity. These changes in the phases of activity are short-lived and require extremely rapid sequences. In order to take advantage of the effect of fast dephasing, T2W FSE sequences are used for the 1.5T and 3T field strength magnets for the BOLD technique, from which R2* maps are calculated (Figure 7.) [12].

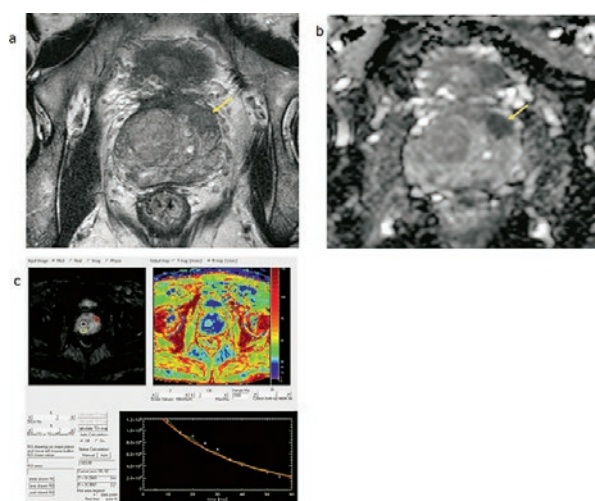


Figure 7. MRI of the prostate T2W (a.), DWI (b.), BOLD (c.)

Source: <https://pubmed.ncbi.nlm.nih.gov/34235962/#&gid=article-figures&pid=figure-1-uid->

T2 mapping

T2 mapping is a technique that allows the quantification of T2W signals. The technique is based on mapping the T2 time of relaxation of prostate tissue. The biophysiological basis for T2 mapping is based on the relative percentages of stromal and glandular tissue, and the water component that varies between benign and cancerous prostate tissue. Using a series of SE sequences, a relaxation curve is obtained and the T2 relaxation time of each voxel can be determined [13,14].

Sathiadoss et al. [15] conducted a study aimed at assessing the image quality and the possibility of detecting prostate cancer by T2 mapping and DWI sequence in men with hip prostheses. The study involved 30 men with hip prostheses, undergoing MRI of the prostate gland read by 5 radiologists, independent of each other. The study showed that images obtained by T2 mapping were of better quality than images of DWI sequences. They concluded that T2 mapping should be included in the MRI of the prostate in men with an implanted hip prosthesis.

Magnetic resonance Fingerprinting (MRF)

MRF is a quantitative imaging technique that enables the rapid and simultaneous generation of T1 and T2 maps

with a unique value of each tissue. The data is collected so that different tissues have unique signal fingerprints. The tissue signal fingerprint database contains a subset of all expected tissue signals generated by simulations. The resulting impressions are compared with simulated impressions from the base (pattern recognition) to identify the tissue under each voxel. Based on the identified tissue from the base, each voxel is assigned a tissue property to generate an impression map (Figure 8.) [16,17]. The advantages of MRF over standard mapping techniques are multi-site repeatability and significantly shorter acquisition time. Given the current trend, shorter acquisition time also allows for shorter imaging protocols, while maintaining the diagnostic quality of the examination [18].

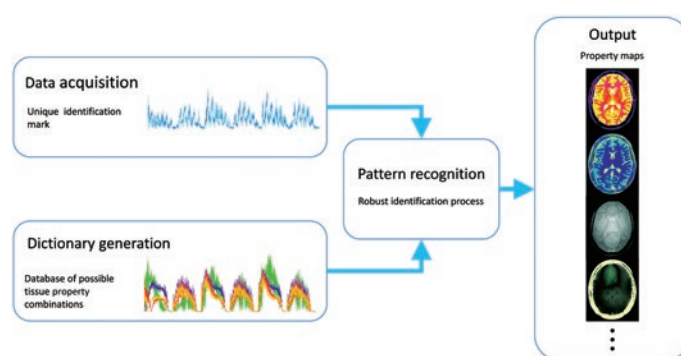


Figure 8. Example of how MRF works

Source: <https://onlinelibrary.wiley.com/cms/asset/6fd61ec4-d3b6-4403-9cbd-d81bce16f50e/mrm27403-fig-0001-m.jpg>

Results

MRI is one of the basic diagnostic tests for detecting pathological conditions of the prostate gland. Thanks to bpMRI and mpMRI protocols, it has found its indispensable place in diagnosing and monitoring prostate cancer, benign prostatic hyperplasia, diagnosing and monitoring inflammatory conditions, conducting targeted prostate cancer biopsies, assessing the effect of radiotherapy and chemotherapy [19]. The basis of the protocol for MRI of the prostate is made up of T2W, DWI and DCE sequences. When imaging the prostate, it is important to clearly distinguish between the central, peripheral and transitional zones. A successful diagnostic test requires the acquisition of high-resolution images and contrast in the shortest possible time without losing their quality. MRI of the prostate gland is recorded on devices with a field strength of 1.5T or 3T. The main advantage of 3T field power devices over 1.5T field power devices is manifested in the field strength that gives a higher SNR. Twice the SNR is obtained by inducing an MR signal in the receiving coil that is proportional to the strength of the main magnetic field (B0) and by noise that has a linear dependence on the strength of the magnetic field > 1.0T. The resulting difference in SNR can be used to reduce search time or increase spatial resolution. The fundamental advantage of MRI 1.5T is the lower sensitivity to metal-induced artifacts in the imaging area (e.g. hip arthroplasty) and the greater range of MRI-conditioned medical devices, primarily pacemakers [20].

Table 1. Sequence parameters for MR 1.5T and MR 3T [21]

| Parameters | Axial T2W TSE | | Axial DWI | |
|---------------------------|------------------------|------------------------|------------------------|------------------------|
| | 1.5T | 3T | 1.5T | 3T |
| Coil | 6-channel phased-array | 6-channel phased-array | 6-channel phased-array | 6-channel phased-array |
| TR(ms)/TE (ms) | 10130/113 | 10630/117 | 4800/93 | 4600/90 |
| Voxel size (mm) | 0.7 x 0.7 x 3.0 | 0.5 x 0.5 x 3.0 | 1.5 x 1.5 x 3.0 | 1.5 x 1.5 x 3.0 |
| Gap (%) | 10 | 10 | 10 | 10 |
| Field of View (mm) | 128 | 128 | 204 | 204 |
| Matrix | 192x192 | 256x256 | 136x136 | 136x136 |
| Number of Signal averages | 3 | 2 | 9 | 8 |
| b-values | | | 0, 500, 1000 | 0, 500, 1000 |
| Number of slices | 30 | 30 | 30 | 30 |
| Acquisition Time | 8:48 | 8:21 | 5:18 | 4:31 |

From the first issuance of the PI-RADS guidelines in 2015 until today, the guidelines state that 1.5T and 3T field strength MRI devices can provide adequate and reliable MRI of the prostate. Nonetheless, the majority of PI-RADS Board members prefer, use, and recommend that prostate MRI be performed on 3T field strength devices.

Taking all this into account, Ulrich et al. [21] conducted a study comparing the quality of MRI images of the prostate on 1.5T and 3T field strength devices. The primary objective of the study was to prove that the SNR and CNR between MR 1.5T and MR 3T when performing T2W and DWI sequences is equal to or less than 10%. The secondary objectives of the study were to evaluate the subjective assessment of image quality, using a rating scale of 1 to 5, and then to score according to PI-RADS v.2. This assessment refers to benign prostate lesions and prostate cancer and the definition of different prostate zones. The study included 63 patients with elevated PSA

levels referred for MRI of the prostate. It was carried out in the period from September 2013 to May 2014. All patients underwent mpMRI on MRI 3T and bpMRI on MRI 1.5T (maximum interval 33 days) 7 days apart. No intervention was made between the two examinations. After mpMRI, 59 patients underwent prostate biopsy and the samples were histopathologically evaluated.

The mpMRI protocols of the prostate were performed on a 3T MRI scanner (Magnetom Trio A TIM System, Siemens Healthcare GmbH), and bpMRI examinations on a 1.5T MRI scanner (Magnetom Avanto, Siemens Healthcare GmbH). Six-channel phase coils for the body were used on both devices. BpMRI on MRI 1.5T was done to avoid unnecessary administration of contrast medium to the patient, since temporal, not spatial, resolution is crucial for DCE. In order to obtain the best image quality for each MRI and for each sequence, the parameters are optimized. (Table 1.) The images did not contain information on which device

Table 2. SNR and CNR values on 3T and 1.5T devices, with statistically significant differences in bold [21]

| Signal-Noise-Ratio (SNR) (mean±SD) | | | 3T | 1.5T | p-value |
|--------------------------------------|---------------------|--------------|---------|---------|---------|
| T2W | Muscle | 1.4±0.4 | 1.4±0.3 | 0.7 | |
| | Prostate | 8.5±2.5 | 8.5±2.6 | 0.9 | |
| | PC | 5.9±2.5 | 6.0±1.8 | 0.7 | |
| DWI | High b-value images | Muscle | 11±1.8 | 7.9±1.4 | <0.001 |
| | | Prostate | 16±2.1 | 11±1.4 | <0.001 |
| | | PC | 20±4.4 | 14±2.5 | <0.001 |
| | ADC map | Muscle | 1.4±0.5 | 1.2±0.3 | 0.03 |
| | | Prostate | 12±2.9 | 9.0±2.0 | <0.001 |
| | | PC | 7.3±3.0 | 6.4±1.7 | 0.2 |
| Contrast-Noise-Ratio (CNR) (mean±SD) | | | 3T | 1.5T | p-value |
| T2W | Prostate-PC | 2.3±1.7 | 2.7±2.5 | 1 | |
| | PZ-TZ | 2.6±2.0 | 2.7±2.2 | 0.8 | |
| DWI | High b-value images | Prostate -PC | 4.1±3.2 | 2.1±1.8 | 0.05 |
| | | PZ-TZ | 0.8±0.8 | 0.4±0.4 | <0.001 |
| | ADC map | Prostate -PC | 3.7±2.4 | 3.0±1.8 | 0.4 |
| | | PZ-TZ | 1.9±1.8 | 1.4±1.3 | 0.2 |

they were taken and were evaluated by two independent radiologists (R1 and R2).

The primary objective of the study showed that differences in normalized signal strength (nSI) in T2W and in ADC maps obtained on MRI 3T and MRI 1.5T were not statistically significant for ROI in prostate cancer lesions or for ROI in benign prostate tissue. In images with a high b-value, there were significant differences between the nSI data obtained MR 3T and MR 1.5T measured for ROI in the whole prostate and peripheral and transition zone (MR 3T: $nSI = 1.3 \pm 0.5$ and MR 1.5T: $nSI = 1.2 \pm 0.1$). In the obtained T2W images, there was no significant difference in SNR between MR 3T and MR 1.5T for ROI in muscle (lat. m. obturator internus) and prostate, regardless of the localization of prostate cancer in the peripheral or transition zone (Table 2).

Significant differences between MR 3T and MR 1.5T were measured in images with a high b-value for all selected ROIs in muscle, prostate and prostate cancer. In the ADC maps, the SNR varied significantly for muscle and the entire prostate. For SNR measurements in ADC maps, ROI was set exclusively in prostate cancer lesions

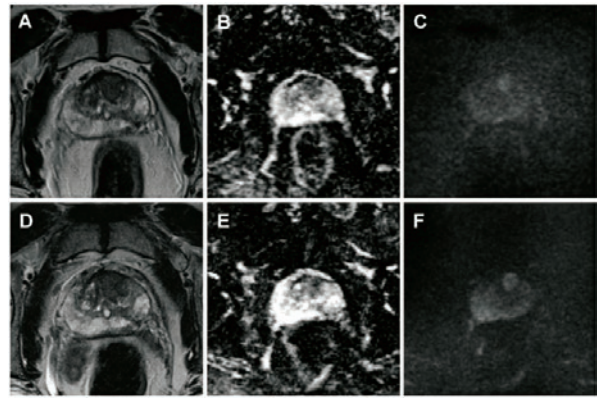


Figure 9. An example of the quality of the images used in the research. Images of A (T2W), B (ADC map) and C (DWI) obtained on MRI 1.5T and D (T2W), E (ADC map) and F (DWI) obtained on MRI 3T. High b-value images (1000 s/mm²) obtained on the 3T MRI (F) are qualitatively superior to the obtained image on the 1.5T MRI.

Source: <https://www.sciencedirect.com/science/article/pii/S0720048X17300967#fig0005>

Table 3. Subjective quality (scale 1-5) and PI-RADS v2. evaluation by two radiologists (R1, R2) for images collected on MRI 3T and MRI 1.5T [21]

| Subjective IQ (mean \pm SD) | | | 3T | 1.5T | p-value |
|-------------------------------|---------|---------------------|---------------|---------------|------------------|
| Patients | | | 63 | 63 | MWU |
| R1 | T2W | | 4.2 \pm 1.0 | 3.8 \pm 0.8 | 0.01 |
| | DWI | High b-value images | 4.1 \pm 0.8 | 3.5 \pm 0.8 | <0.001 |
| | | ADC map | 4.1 \pm 0.7 | 3.8 \pm 0.6 | 0.01 |
| R2 | T2W | | 4.2 \pm 0.9 | 3.8 \pm 0.8 | 0.01 |
| | DWI | High b-value images | 4.2 \pm 0.8 | 3.6 \pm 0.8 | <0.001 |
| | | ADC map | 4.2 \pm 0.7 | 3.9 \pm 0.6 | 0.01 |
| PI-RADS Score (mean \pm SD) | | | 3T | 1.5T | p-value |
| R1 | T2W | | 2.9 \pm 1.0 | 2.9 \pm 1.0 | 0.8 |
| | DWI | | 2.9 \pm 1.0 | 2.8 \pm 1.0 | 0.2 |
| | Overall | | 3.3 \pm 1.0 | 3.3 \pm 1.0 | 0.7 |
| R2 | T2W | | 3.0 \pm 0.9 | 3.0 \pm 0.9 | 1 |
| | DWI | | 3.9 \pm 0.9 | 3.9 \pm 0.9 | 0.7 |
| | Overall | | 3.4 \pm 1.0 | 3.4 \pm 0.9 | 0.9 |
| PI-RADS Score (PCa) n = 15 | | | | | |
| R1 | T2W | | 4.4 \pm 0.8 | 4.4 \pm 0.8 | 1 |
| | DWI | | 4.5 \pm 0.7 | 4.3 \pm 0.8 | 0.5 |
| | Overall | | 4.5 \pm 0.6 | 4.5 \pm 0.6 | 1 |
| R2 | T2W | | 4.3 \pm 0.8 | 4.3 \pm 0.8 | 0.9 |
| | DWI | | 4.4 \pm 0.7 | 4.4 \pm 0.7 | 0.9 |
| | Overall | | 4.5 \pm 0.6 | 4.4 \pm 0.6 | 0.8 |
| PI-RADS Score (benign) n = 44 | | | | | |
| R1 | T2W | | 2.6 \pm 0.8 | 2.7 \pm 0.7 | 0.7 |
| | DWI | | 2.6 \pm 0.7 | 2.5 \pm 0.7 | 0.05 |
| | Overall | | 2.9 \pm 0.8 | 2.8 \pm 0.8 | 0.6 |
| R2 | T2W | | 2.7 \pm 0.7 | 2.7 \pm 0.7 | 0.9 |
| | DWI | | 2.7 \pm 0.7 | 2.7 \pm 0.7 | 0.6 |
| | Overall | | 3.0 \pm 0.8 | 3.0 \pm 0.7 | 1 |

| Author | Number | 3.0 T scanner | 3.0 T MRI sequences | 1.5 T scanner | 1.5 T MRI sequences | Objective | Subjects and primary findings |
|------------------|--------------------------|--|---|---|---|--|---|
| Beyersdorff [14] | 22 | Signa 3.0 T (GE Healthcare) using a torso phased-array coil (USA Instruments) | After a localizer scan, at least a T2W angulated axial FSE sequence with a TR/TE of 4,500/102 and an ETL of 8 or 16 and an angulated coronal FSE sequence (3,800/78.3; ETL, 8) with a FOV of 16 × 16 cm and a matrix of 256 × 256 were acquired. Four acquisitions were performed with each sequence at a slice thickness of 4 mm and a gap of 1 mm*. | Magnetom Vision or Magnetom Symphony (Siemens Medical Solutions) using a combination of an endorectal coil (Medrad) and a body phased-array coil. | T2W TSE sequence in angulated axial (3,500/96; ETL, 13; 3 acquisitions) and coronal (4,522/112; ETL, 13; 2 acquisitions) slice orientations with a FOV of 16 × 16 cm. The matrix was 256 × 256. In addition, an angulated axial T1W spin-echo sequence (680/14; ETL, 3) was acquired. The FOV was 16 × 16 cm, and the matrix was 256 × 256. The slice thickness was 3 mm and the interslice gap, 0.9 mm*. | To compare the image quality, tumour delineation, and depiction of staging criteria on MRI of PCa at 1.5 and 3.0 T. | No statistically significant differences in the visualization of staging criteria. |
| Torricelli [15] | 29 | Intera 3.0 T magnet, operating at 3.0 T (Philips Medical System), using a 6-channel external phased-array cardiac receiver coil | TSE T2W (TR/TE: 5504/120 ms) in the axial and coronal plane with ETL: 21, NSA: 4, FOV: 210 mm, slice thickness: 3 mm, gap: 0.5 mm, scan matrix: 320 × 320, and scan reconstruction: 512 × 512. TSE T1w (TR/TE: 445/11 ms) in the axial plane with ETL: 3, NSA: 2, FOV: 210 mm, slice thickness: 3 mm, gap: 0.5 mm, scan matrix: 320 × 320, and scan reconstruction: 512 × 512. | Intera 1.5 T Philips magnet, operating at 1.5 T (Philips Medical System), using an Eccia 64 MHz endocavitary coil (Philips Medical System). | TSE T2W (TR/TE: 4750/130 ms) in the axial and coronal plane with ETL: 18, NSA: 6, FOV: 180 mm, slice thickness: 3 mm, gap: 0.5 mm, scan matrix: 320 × 320, and reconstruction matrix: 512 × 512. TSE T1W (TR/TE: 445/11 ms) in the axial plane with ETL: 3, NSA: 2, FOV: 180 mm, slice thickness: 3 mm, gap: 0.5 mm, scan matrix: 320 × 320, and reconstruction matrix: 512 × 512. | To compare the image quality and the diagnostic accuracy of endorectal coil 1.5 T MRI and phased-array coil 3.0 T MRI in staging of PCa. | 3.0 T MRI had worse image quality but can provide similar diagnostic information compared with 1.5 T MRI. |
| Park [13] | 108 | Intera Achieva 3.0 T (Philips Medical System); examination was performed using a 6-channel external phased-array cardiac receiver coil (USA Instruments) | TSE using a SENSE technique (factor = 2) was used for T2W imaging with the following parameters: TR, 3300 to 4000 ms; TE, 80 to 100 ms; TSE factor, 12; FOV, 15 cm (17 cm for sagittal images); matrix number, 304 × 304; one acquisition; slice thickness, 3 mm; gap, 0.3 mm. Second, axial T1W imaging in a large FOV (24 cm) at both 3.0 and 1.5 T.** | Genesis Signa; GE Healthcare with endorectal coil (Medrad). | FSE was used for T2W imaging with the following parameters: TR, 3300-4000 ms; TE, 80-100 ms; ETL, 13; FOV, 18 cm; matrix number, 512 × 256; one acquisition; slice thickness, 3 mm; gap, 1 mm. Second, axial T1W imaging in a large FOV (24 cm) at both 3.0 and 1.5 T.** | To evaluate local staging accuracy for PCa at 3.0 T MRI compared with 1.5 T MRI. | 3.0 T phased-array MRI is equivalent to the 1.5 T endorectal MRI in evaluating local staging accuracy for PCa without significant loss of imaging quality. |
| Ryznarova [16] | 103 (1.5 T: 41, 3 T: 63) | Trio, Siemens, using 8-channel phased-array surface coils. | T1W TSE sequence in axial plane T2W TS sequences were performed in axial (orthogonal to the urethra), coronal, and sagittal planes. Echo-planar DWI was obtained in transverse plane parallel to the transverse T2W to construct ADC maps using the standard Siemens software. DCE 3D T1-spoiled gradient echo images were acquired during an intravenous bolus injection of paramagnetic contrast medium (gadobenate dimeglumine) at a dose of 0.1 mmol/kg of body weight for examination at 3.0 T. A MRS was also obtained by using a point-resolved 3D spectroscopic imaging sequence. | Avanto Siemens, Erlangen, Germany using 8 channels phased-array surface coils. | T1W TSE sequence in axial plane; T2W TSE sequences were performed in axial (orthogonal to the urethra), coronal, and sagittal planes. Echo-planar DWI was obtained in transverse plane parallel to the transverse T2W to construct ADC maps using the standard Siemens software. DCE 3D T1-spoiled gradient echo images were acquired during an intravenous bolus injection of paramagnetic contrast medium (gadobenate dimeglumine) at a dose of 0.2 mmol/kg of body weight for examination at 1.5 T. MRS was also obtained by using a point-resolved 3D spectroscopic imaging sequence. | To compare the results of MRI obtained by the 1.5 T and 3.0 T scanners using surface coils in patients with PCa. | Highest accuracy of local PCa staging with 3.0 T MRI scanner was seen when the protocol included DCE. No significant difference was found in tumour localization assessment between 3.0 T and 1.5 T MRI scanners. |

Figure 10. An overview of accepted studies with their characteristicsSource: <https://www.ncbi.nlm.nih.gov/pmc/articles/PMC9373864/table/T1/?report=objectonly>

and did not differ significantly between MR 3T and MR 1.5T. For CNR measurements on MRI 3T and MRI 1.5T T2W sequences and ADC maps, ROI was set in benign prostate tissues and prostate cancer lesions. In high-b-value images, the CNR for ROI placed in benign prostate tissue and prostate cancer lesions was 4.1 ± 3.2 on MRI 3T and 2.1 ± 1.8 on MRI 1.5T. For the peripheral and transition zones, the 3T MRI was 0.8 ± 0.8 , and 0.4 ± 0.4 respectively on the 1.5T MRI. Therefore, with sequence optimization on both MR 1.5T and MRI 3T, images of approximate SNR

and CNR values can be obtained. (Table 3). For both radiologists, the average subjective image quality (Figure 9.) estimated on a scale of 1 to 5 was significantly better for the T2W sequence on MRI 3T compared to the sequence on MRI 1.5T ($R1: 4.2 \pm 1.0$ and 3.8 ± 0.8 , respectively; $R2: 4.2 \pm 0.9$ and 3.8 ± 0.8), as well as for high-b-value images ($R1: 4.1 \pm 0.8$ and 3.5 ± 0.8 , $R2: 4.2 \pm 0.8$ and 3.6 respectively ± 0.8) and ADC maps ($R1: 4.1 \pm 0.7$ and 3.8 ± 0.6 , respectively; $R2: 4.2 \pm 0.7$ and 3.9 ± 0.6 , respectively). (Table 3.)

A total of 170 MRI lesions were defined for PI-RADS assessment. The individual results of both radiologists according to the PI-RADS classification for T2W and DWI images obtained on MRI 3T and MRI 1.5T were similar to the overall result in both radiologists. Patients with prostate cancer had significantly higher PI-RADS scores compared to patients with benign histopathological findings (total PI-RADS scores of 4.5 ± 0.6 and 2.9 ± 0.8 for R1 and 4.5 ± 0.6 and 3.0 ± 0.8 for R2, respectively). (Table 3.)

Although subjectively the quality of the images was rated significantly better on MRI 3T for all imaging sequences and in both radiologists, PI-RADS scoring was similar for MR 3T and MR 1.5T. None of the patients diagnosed with histologically proven prostate cancer received a total PI-RADS score below 4, either with images obtained on 3T MRI or 1.5T MRI.

In July 2022, Virarkar et al. [22] published a systematic review of studies with a meta-analysis aimed at determining the optimal field strength for prostate cancer MRI. The initial search yielded 24 articles and after applying the given selection criteria, 8 of them were reviewed. Of these, 4 studies included MRI of prostate cancer at both 3T and 1.5T and were selected for the study. All studies found a low risk of systemic bias in participant selection, except in Parker's study. The study by Torricelli et al. did not identify a low risk of systemic error for reference standards. All studies were rated as low risk for flow, time and index test. For MR 3T, the group sensitivity was 69.5%, with a 95% confidence interval (CI) of 56.4 to 80.1%. The group specificity for MR 3T was 48.8%, with a 95% CI of 6 to 93.4%. The group diagnostic odds ratio (DOR) for MRI 3T was 3%, with a 95% CI of 0 to 26%. The area under the curve (AUC) was 0.684. The collective sensitivity for MR 1.5T was 70.6%, with a 95% CI of 55.0 to 82.5%. The group sensitivity for MR 1.5T was 70.6%, with a 95% CI of 55.0 to 82.5%. The group specificity for MR 1.5T was 41.7%, with a 95% CI of 6.2 to 88.6%. The group DOR for MR 1.5T was 2, with a 95% confidence interval of 0 to 18. AUC was 0.679. (Figure 10.)

A meta-analysis of MRI comparison on 3T and 1.5T field strength devices for determining the stage of pros-

tate cancer did not find significant relationships between magnet strength, sensitivity, specificity, or DOR values ($p = 0.91, 0.88, \text{ and } 0.89$, respectively). (Figure 11.)

Conclusion

Prostate cancer is the second most common cancer in the male population in the world and the fifth most fatal. Despite the fact that PI-RADS recommendations state that MRI of the prostate is performed on 3T power devices, more and more studies emphasize the equal diagnostic value of prostate MRI on 1.5T devices in diagnosing and monitoring diseases. The study was limited by the small amount of available studies comparing the quality of prostate MRI with 1.5T and 3T field strength devices, but monitoring over a 10-year period, from 2012 to 2022, can conclude that there was a significant improvement in the quality of 1.5T field strength devices. By comparing studies, it was found that due to SNR, sequences, primarily DWI, have technically better performance, but without a significant diagnostic difference in the detection of prostate cancer compared to MRI performed on 1.5T devices. By introducing 3D and MRF sequences, we can further shorten the duration of prostate MRI, and by introducing BOLD sequences, T2 mapping and MRF sequences, we can quantify the signal and get a better ability to assess the spread of prostate cancer, as well as improve differentiation in relation to BPH and prostatitis. As mentioned at the beginning, the relatively small proportion of comparative studies of MR 1.5T and MR 3T, the absence of analysis of other parameters that affect the quality of the sequence (matrix size, bandwidth, additional analysis of coil selection, FOV selection, etc.) and the heterogeneity of the studies require that the results of this meta-analysis be taken with a grain of salt.

Taking into account the above, further research is needed in this area to determine whether the diagnostic value of MRI of the prostate depends on the strength of the magnetic field.

All data in this paper are part of the results from the master's thesis titled "Comparison of magnetic resonance imaging of the prostate 1.5T and 3T", written at the University Department of Health Studies, University of Split [23].

| Parameter | 3.0 T | 1.5 T | P |
|----------------------|-----------------------|------------------------|------|
| TP | 68 | 67 | - |
| TN | 47 | 28 | - |
| FP | 19 | 21 | - |
| FN | 26 | 23 | - |
| Sensitivity (95% CI) | 69.5% (56.4-80.1%) | 70.6% (55.0- 82.5%) | 0.91 |
| Specificity (95% CI) | 48.8% (6.0-93.4%) | 41.7% (6.2-88.6%) | 0.88 |
| DOR (95% CI) | 3 (0-26) | 2 (0-18) | 0.89 |
| AUC | 0.684 | 0.679 | - |

Figure 11. Results of a meta-analysis of diagnostic efficacy of 3.0 T versus 1.5 T MRI in determining the stage of prostate cancer

Source: <https://www.ncbi.nlm.nih.gov/pmc/articles/PMC9373864/table/T3/?report=objectonly>

Literature:

1. PI-RADS v2.1. (preuzeto 12.2.2023.) Dostupno na <https://www.acr.org/-/media/ACR/Files/RADS/PI-RADS/PI-RADS-v2-1.pdf>
2. Giganti F., Rosenkrantz B. A., Villeirs G., Panebianco V., Stabile A., Emberton M., Moore C. M. The Evolution of MRI of the Prostate: The Past, the Present, and the Future. *AJR Am J Roentgenol.* 2019 Aug; 213(2): 384-396.
3. Giganti F., Allen C. Imaging quality and prostate MR: it is time to improve. *Br J Radiol.* 2021 Feb 1;94(1118):20200934. doi: 10.1259/bjr.20200934.
4. Westbrook C., Talbot J. MRI in Practice, 5th Edition. Wiley-Blackwell, 2018.
5. Jambor I. Optimization of prostate MRI acquisition and post-processing protocol: a pictorial review with access to acquisition protocols. *Acta Radiol Open.* 2017 Dec 8;6(12):2058460117745574. doi: 10.1177/2058460117745574.

6. Maier SE, Wallström J, Langkilde F, Johansson J, Kuczer S, Hugosson J, Hellström M. Prostate Cancer Diffusion-Weighted Magnetic Resonance Imaging: Does the Choice of Diffusion-Weighting Level Matter? *J Magn Reson Imaging*. 2022 Mar;55(3):842-853. doi: 10.1002/jmri.27895.
7. Tamada T, Kido A, Ueda Y, Takeuchi M, Fukunaga T, Sone T, Yamamoto A. Clinical impact of ultra-high b-value (3000 s/mm²) diffusion-weighted magnetic resonance imaging in prostate cancer at 3T: comparison with b-value of 2000 s/mm². *Br J Radiol*. 2022 Mar 1;95(1131):20210465. doi: 10.1259/bjr.20210465.
8. Polanec SH, Lazar M, Wengert GJ, Bickel H, Spick C, Susani M, Shariat S, Clauser P, Baltzer PAT. 3D T2-weighted imaging to shorten multiparametric prostate MRI protocols. *Eur Radiol*. 2018 Apr;28(4):1634-1641. doi: 10.1007/s00330-017-5120-5.
9. Vidya Shankar R, Rocca E, Cruz G, Neji R, Botnar R, Prezzi D, Goh V, Prieto C, Dregely I. Accelerated 3D T2 w-imaging of the prostate with 1-millimeter isotropic resolution in less than 3 minutes. *Magn Reson Med*. 2019 Aug;82(2):721-731. doi: 10.1002/mrm.27764.
10. Caglic I, Povalej Brzan P, Warren AY, Bratt O, Shah N, Barrett T. Defining the incremental value of 3D T2-weighted imaging in the assessment of prostate cancer extracapsular extension. *Eur Radiol*. 2019 Oct;29(10):5488-5497. doi: 10.1007/s00330-019-06070-6.
11. Alonzi R, Taylor NJ, Stirling JJ, d'Arcy JA, Collins DJ, Saunders MI, Hoskin PJ, Padhani AR. Reproducibility and correlation between quantitative and semiquantitative dynamic and intrinsic susceptibility-weighted MRI parameters in the benign and malignant human prostate. *J Magn Reson Imaging*. 2010 Jul;32(1):155-64. doi: 10.1002/jmri.22215.
12. Kim Y, Park JJ, Kim CK. Blood oxygenation level-dependent MRI at 3T for differentiating prostate cancer from benign tissue: a preliminary experience. *Br J Radiol* 2022; 95: 20210461.
13. Klingebiel M, Schimmöller L, Weiland E, Franiel T, Jannusch K, Kirchner J, Hilbert T, Strecker R, Arsov C, Wittsack HJ, Albers P, Antoch G, Ullrich T. Value of T2 Mapping MRI for Prostate Cancer Detection and Classification. *J Magn Reson Imaging*. 2022 Aug;56(2):413-422. doi: 10.1002/jmri.28061.
14. Mai J, Abubrig M, Lehmann T, Hilbert T, Weiland E, Grimm MO, Teichgräber U, Franiel T. T2 Mapping in Prostate Cancer. *Invest Radiol*. 2019 Mar;54(3):146-152. doi: 10.1097/RLI.0000000000000520.
15. Sathiadoss P, Schieda N, Haroon M, Osman H, Alrasheed S, Flood TA, Melkus G. Utility of Quantitative T2-Mapping Compared to Conventional and Advanced Diffusion Weighted Imaging Techniques for Multiparametric Prostate MRI in Men with Hip Prosthesis. *J Magn Reson Imaging*. 2022 Jan;55(1):265-274. doi: 10.1002/jmri.27803.
16. Al-Bourini O, Seif Amir Hosseini A, Giganti F, Balz J, Heitz LG, Voit D, Lotz J, Trojan L, Frahm J, Uhlig A, Uhlig J. T1 Mapping of the Prostate Using Single-Shot T1FLASH: A Clinical Feasibility Study to Optimize Prostate Cancer Assessment. *Invest Radiol*. 2022 Dec 8. doi: 10.1097/RLI.0000000000000945.
17. Sushentsev N, Kaggie JD, Slough RA, Carmo B, Barrett T. Reproducibility of magnetic resonance fingerprinting-based T1 mapping of the healthy prostate at 1.5 and 3.0 T: A proof-of-concept study. *PLoS One*. 2021 Jan 29;16(1):e0245970. doi: 10.1371/journal.pone.0245970.
18. Shiradkar R, Panda A, Leo P, Janowczyk A, Farre X, Janaki N, Li L, Pahwa S, Mahran A, Buzzy C, Fu P, Elliott R, MacLennan G, Ponsky L, Gulani V, Madabhushi A. T1 and T2 MR fingerprinting measurements of prostate cancer and prostatitis correlate with deep learning-derived estimates of epithelium, lumen, and stromal composition on corresponding whole mount histopathology. *Eur Radiol*. 2021 Mar;31(3):1336-1346. doi: 10.1007/s00330-020-07214-9.
19. Tamada T, Kido A, Yamamoto A, Takeuchi M, Miyaji Y, Moriya T, Sone T. Comparison of Biparametric and Multiparametric MRI for Clinically Significant Prostate Cancer Detection With PI-RADS Version 2.1. *J Magn Reson Imaging*. 2021 Jan;53(1):283-291. doi: 10.1002/jmri.27283.
20. Felisi M, Monti AF, Lizio D, Nici S, Pellegrini RG, Riga S, Bortolato B, Brambilla MG, Carbonini C, Abujami M, Carsana C, Sibio D, Potente C, Vanzulli A, Palazzi MF, Torresin A. MRI only in a patient with prostate cancer with bilateral metal hip prostheses: case study. *Tumori*. 2021 Dec;107(6):NP41-NP44. doi: 10.1177/0300891621997549.
21. Ullrich T, Quentin M, Oelers C, Dietzel F, Sawicki LM, Arsov C, Rabenalt R, Albers P, Antoch G, Blondin D, Wittsack HJ, Schimmöller L. Magnetic resonance imaging of the prostate at 1.5 versus 3.0T: A prospective comparison study of image quality. *Eur J Radiol*. 2017 May;90:192-197.
22. Virarkar M, Szklaruk J, Diab R, Bassett R, Bhosale P. Diagnostic value of 3.0 T versus 1.5 T MRI in staging prostate cancer: systematic review and meta-analysis. *Pol J Radiol*. 2022 Jul 29;87:e421-e429.
23. Kutlić G. Usporedba oslikavanja prostate magnetskom rezonancijom 1.5 T i 3 T (Diplomski rad). Split: Sveučilište u Splitu, Sveučilišni odjel zdravstvenih studija; 2023 (pristupljeno 13.01.2025.) Dostupno na: <https://urn.nsk.hr/urn:nbn:hr:176:919786>

Usporedba oslikavanja prostate magnetskom rezonancijom 1.5T i 3T

Sažetak

Izvršnim prikazom mekih tkiva i mogućnostima trodimenzionalnog prikaza magnetska rezonancija od svojih je početaka prije 40 godina do danas postala jedna od temeljnih dijagnostika u prikazu prostate i njezinih patoloških stanja. Iako je veća dostupnost uređaja za magnetsku rezonanciju snage polja 1.5T, preporuka Europskog udruženja urogenitalnih radiologa je da se snimanje prostate magnetskom rezonancijom vrši na uređajima snage polja 3T. Uređaji snage 3T nametnuli su se zbog povećanog omjera signala i šuma (SNR) koji se može iskoristi za skraćivanje vremena snimanja ili povećanja rezolucije, tj. poboljšanja kvalitete slike. Sve je više istraživanja primjene kvantitativnih tehnika, kao što su engl. *Magnetic resonance fingerprinting*, T2 mapiranje, BOLD, kojima bi se mogla poboljšati detekcija i kvantificiranje lezija karcinoma prostate, a optimizacijom protokola na 1.5T i 3T moguće je učiniti pretrage jednake dijagnostičke vrijednosti.

Ključne riječi: MRI; prostata; 1.5T; 3T